Investigation of Displacements Fields Due to Normal and Tangential Loads on Bars of Finite Thickness

B. Trentadue* and G. Illuzzi

Dipartimento Di Meccanica Matematica e Management, Politecnico Di Bari-Viale Japigia, 182-70126, Bari-Italy

Abstract: The challenging topic of a cylinder in line contact with bars of finite thickness, reproducing typical fretting fatigue experiments, is studied by means of the super moiré interferometry technique. The authors consider a normal load on a model producing a contact area of about 4 mm, and subsequently on a tangential load at nearly the sliding limit. The displacement fields, due to the normal load, show that the maximum principal stresses at the edge of the contact area are significantly different from those predicted for the half plane, as well as for bars with a significant thickness, so that the dimension of the contact area and the pressure distribution are nearly the same as those of the half plane. This is confirmed by numerical results obtained by Fellows *et al.* [7].

Moreover, the experimental results show that the surface stresses induced are not as dependent on the thickness of the bar as those induced by the normal load.

Keywords: Moirè interferometry, fretting, fatigue, displacement field, contact.

1. INTRODUCTION

Many fretting-fatigue tests make use of a configuration similar to that shown in Figure **1**. An elastic bar is first compressed between two cylinders, and sequentially loaded under tension from one end. The two cylinders are placed in a frame that is connected to the support of the bar with calibrated springs, so that the bar is simultaneously loaded by tangential forces due to the friction between the two cylinders. This particular configuration was studied by Nowell and Hills [1] assuming, as a first attempt, that the thickness of the bar is much greater than the contact semi-width, i.e. each body could be approximated by a half plane. Analytical solutions of the entire stress field on the half plane are available in the full sliding case (Smith and Liu, [2]), and the two dimensional equivalent of Mindlin [3] solutions is available for the traction distributions in any other case of normal and tangential loading, from which the subsurface stresses can be calculated using, for example, the results of Poritsky [4]. The bulk tension should then be superposed to the subsurface stresses induced by the contact tractions. Nowell and Hills [1] proved that the presence of a bulk tension on the half plane affects the surface tractions, so that they significantly differ from Mindlin ones. In an apparatus as in Figure **1**, moreover, the bulk tension is not constant throughout the specimen, since it actually depends on how the equilibrium is achieved, hence this approach leads to a quite complex coupled problem.

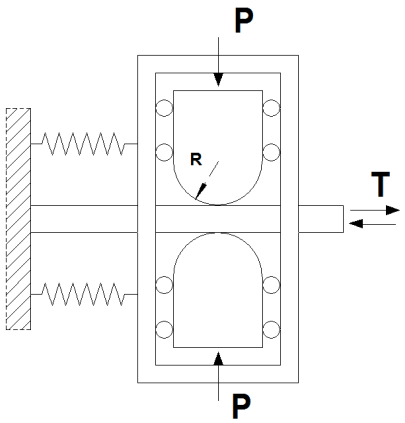

Figure 1: Contact configuration.

Regarding the effect of finite thickness of the bar, several studies using the Fourier transform methods [5, 6] have shown that surface tractions differ only slightly from those of the half plane, provided that the ratio between the thickness of the bar and the contact half width is higher than about five. Even for these ratios, it has been recently demonstrated [7] that in the normal loading case the subsurface stresses predicted for the half plane underestimate the real stress field on the bar. Moreover, in the numerical calculation of the subsurface stress field induced by normal and tangential tractions in the correct finite thickness strip model, the use of Fourier transforms has to be rather cautious, because it is usually very difficult to ensure the correct restraints. Finite or Boundary Elements analysis can be resorted to, but this can be highly time consuming, especially in finding convergence of the incremental and iterative procedures. Therefore, the determination of the surface and then subsurface stress distributions for actual configurations is not an

*Address correspondence to this author at the Dipartimento Di Meccanica Matematica e Management, Politecnico Di Bari - Viale Japigia, 182-70126, Bari–Italy; Tel: +39.080.5962709; Fax: +39.080.5962709;
E-mail: btrentadue@poliba.it; giuseppe.illuzzi@gmail.com

E-ISSN: 2409-9848/15

easy task, so that an experimental investigation, if accurate and reliable, is highly desirable.

2. EXPERIMENTAL PROCEDURE

Amongst the experimental techniques, moiré interferometry [8], and in particular the super-moiré method [9], is chosen in order to determine displacement fields resulting from the localized contact. This well known technique gives direct measurement of the in-plane displacement field, with a high sensitivity ($1/2f_s$ if f_s is the grating frequency) and an excellent contrast. This technique has been used by several authors, including ourselves (e.g. [10]), for studying frictional contact problems. The use of moiré interferometry in the problem of a bar clamped between two cylinders and pulled from one extremity is studied, for a contact area having a fixed half width 'a' of about 4 mm, and bars having a thickness 'b' equal to 10 or 20 or 250 mm respectively (Figure **2**).

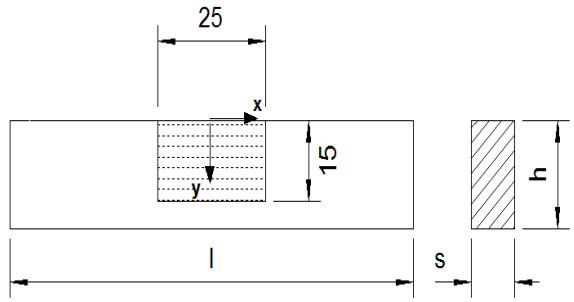

Figure 2: Specimens.

The specimens are made of Plexiglas, with relevant measured mechanical properties equal to: Young modulus E=3400 N/mm^2; Poisson's ratio ν=0.28, yielding strength σ_y=40 N/mm^2 (Figure **2**). Gratings with sensitivity 0.5μm(=$1/2f_s$) are replicated onto the specimens. Real time images are taken by a CCD camera and treated with a PC image processing system.

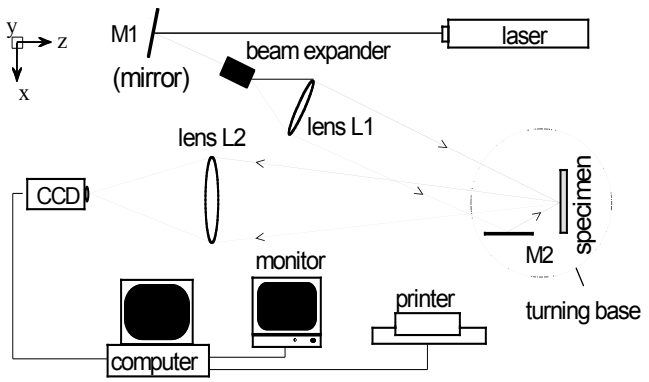

Figure 3: Experimental set-up.

Figure **3** shows the experimental set-up. A collimated beam strikes onto the specimen surface in an incident angle α with z-axis and a mirror M2 is used to provide a symmetrical incident beam. The fringe patterns are recorded into an image processing system in a personal computer through a CCD-camera in real time. The rig is made of four columns built in a rigid base. The specimens are a semi-cylinder and bars of different thickness, guided through the columns. In order to reproduce the symmetry of the system, a semi-cylinder is in contact with a bar placed on a rigid base, and anti-friction material is put between the bar and the rigid base (Figure **4**). The normal load is applied by means of a lever and the tangential load is applied on the cylinder by means of a micrometric screw aligned with the horizontal guides. In order to measure the normal and tangential loads, loading cells are used. With a normal load P of 360 N, the hertzian semi-width of contact area is:

$$a = \sqrt{\frac{8 \cdot P \cdot R}{\pi \cdot E/(1-\upsilon^2)}} \cong 1.8mm \qquad (1)$$

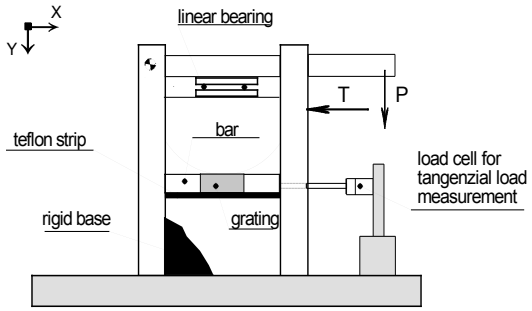

Figure 4: Loading rig.

The tangential load T is 60 N in order to approach the sliding limit (μ=0.2). Table **1** shows the dimensions of the specimens (see symbols in Figure **2**).

Table 1: Main Specimen Dimensions

Specimen	h [mm]	l [mm]	s [mm]	R [mm]
1	20	170	10	-
2	10	170	10	-
half-plane	250	280	10	-
disk	-	-	10	135

3. THEORY

To better compare the results obtained in the experimental analysis, the experiments were

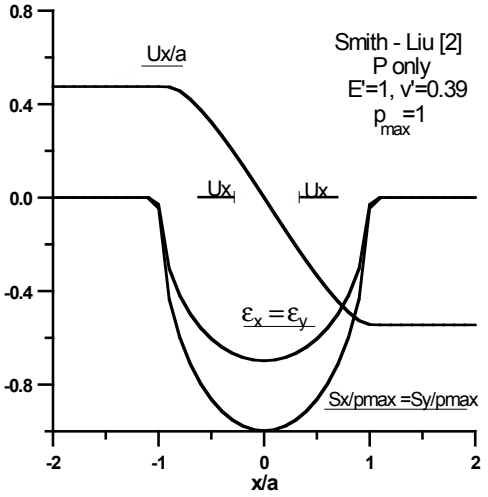

(**a**)

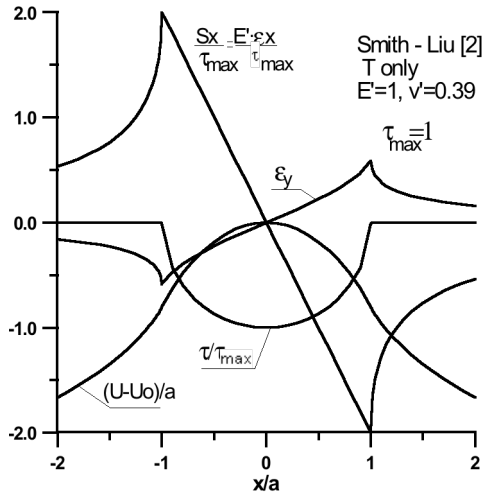

(**b**)

Figure 5: Smith and Liu solution [2].

conducted in order to approach the sliding limit as much as possible. In these conditions, the tangential traction distribution is nearly proportional to the applied pressure, which is hertzian for all the specimens and loading conditions in the present work, so that the half plane reference case studied by Smith and Liu [2] can be considered. The main features of their solution are shown in an adimensional form for the normal and the tangential loading in Figures **5a** and **5b** respectively, and limiting the interest to the surface of the bar, because in this zone the significant differences of the displacements and of the stresses will be disclosed for the bars. Considering the analytical expression of the surface stresses [11]:

$$\sigma_x = \sigma_y = -p_{\max}\sqrt{1-\left(\frac{x}{a}\right)^2}\,;\varepsilon_x = \frac{1-\nu'}{E'}\sigma_x;\ |x/a| \le 1 \qquad (2)$$

the U displacements are obtained as follows:

$$\frac{U}{a} = -p_{\max}\frac{1-\nu'}{E'}\left[\frac{a\sin(x/a)}{2} + \frac{x/a\cdot\sqrt{1-(x/a)^2}}{2}\right] \quad |x/a| \le 1$$
$$\frac{U}{a} = -p_{\max}\frac{1-\nu'}{E'}\frac{\pi}{4}\cdot\mathrm{sgn}(x) \quad |x/a| > 1 \qquad (3)$$

In the case of tangential load, the peak values of σ_x are equal to the double of the maximum tangential traction. The U pattern is parabolic within the loaded zone and progressively decreasing out of it, as follows:

$$\sigma_x = -2\cdot\tau_{\max}\frac{x}{a};\qquad |x/a| \le 1\ ;$$
$$\sigma_x = -2\cdot\tau_{\max}\left[\frac{x}{a} - \sqrt{\left(\frac{x}{a}\right)^2 - 1}\right],\qquad |x/a| > 1 \qquad (4)$$
$$\sigma_y = 0;\quad \varepsilon_x = \frac{1}{E'}\quad \sigma_x;$$

the U displacements respect to the displacement U_0 of the center of the contact area are:

$$\frac{U-U_0}{a} = -2\cdot\tau_{\max}\frac{1}{E'}\left[\frac{(x/a)^2}{2}\right],\quad |x/a| \le 1$$
$$\frac{U-U_0}{a} = -\ln\left[\sqrt{\left(\frac{x}{a}\right)^2 - 1} + \left|\frac{x}{a}\right|\right] + \left|\frac{x}{a}\right|\sqrt{\left(\frac{x}{a}\right)^2 - 1} - \left(\frac{x}{a}\right)^2 \quad |x/a| > 1 \qquad (5)$$

As for the normal displacement in the hertzian contact, the U displacements due to the tangential load can only be given in terms of difference respect to displacements of a reference point.

The relation between displacement fields may be found in:

$$\frac{U_T}{T} = -\frac{V_P}{P};\qquad \frac{V_T}{T} = \frac{U_P}{P} \qquad (6)$$

Another useful reference case is the St. Venant beam subjected to opposite normal concentrated loads on its surfaces [12]. In this case the U displacements are given by:

$$\delta = \nu \frac{P}{E} \tag{7}$$

This means that the displacement due to concentrated compressive forces tends to elongate the beam, whilst the surface displacements in the half plane occur in the opposite direction. When the thickness of the bar decreases, the remote U displacements, directed toward the center of the loaded area for the half plane case, gradually decrease, change direction and approach the value given by the expression (2).

4. RESULTS

The fringes of the displacements U and V due to the normal load in the specimen used to simulate the "half-plane" are shown in Figure **6a**. The surface displacements, shown in Figure **5a** and **5b**, are well correlated to the analytical solution. Note that this solution gives out of the contact area a constant value of the U surface displacements. This is difficult to work out because the fringes are very close to the surface of the specimen. If this comparison is based on the V displacements due to the tangential load, proportional to the U displacements due to normal load (as shown in equation (6)), the correspondence with theoretical behavior is more evident. The theoretical value of the maximum displacement directed toward the contact area is 2.97 μm for the load and the material properties considered in the experimental study (E'=3700 N/mm^2, ν'=0.39). This value is very close to the maximum U displacement obtained in the experiment.

The fringes of the displacements U and V due to the normal load in the specimens 1 and 2 are shown in the Figures **6b** and **6c** respectively. The images are centered on the right of the contact area because of the symmetry properties and the analysis can therefore be performed on a wider area. The effect of bar thickness clearly stems from the patterns of the surface displacements of the U field of the specimens as shown in Figure **7a**. As the thickness reduces, a larger area with tensile strains develops at the end of the contact area. This happens because the displacements U for a finite thickness bar under normal contact loads, with reference to the half plane behavior, is no longer constant out of the contact area.

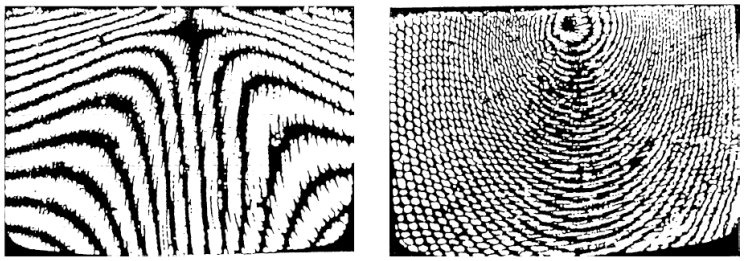

(**a**)

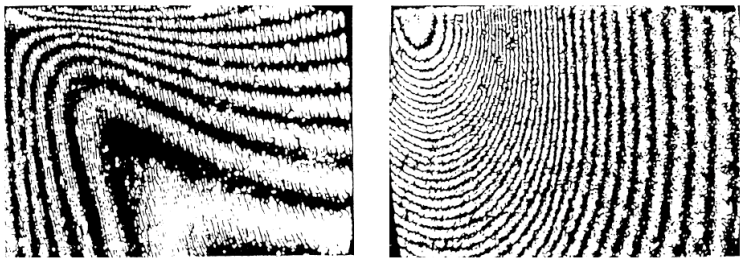

(**b**)

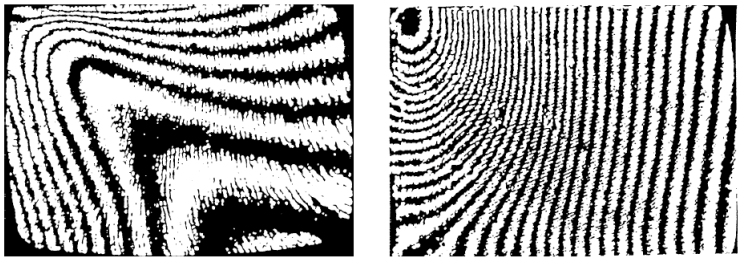

(**c**)

Figure 6: The displacements U and V due to the normal load (**a**) 'half plane' specimen, (**b**)'1' specimen, (**c**) '2' specimen.

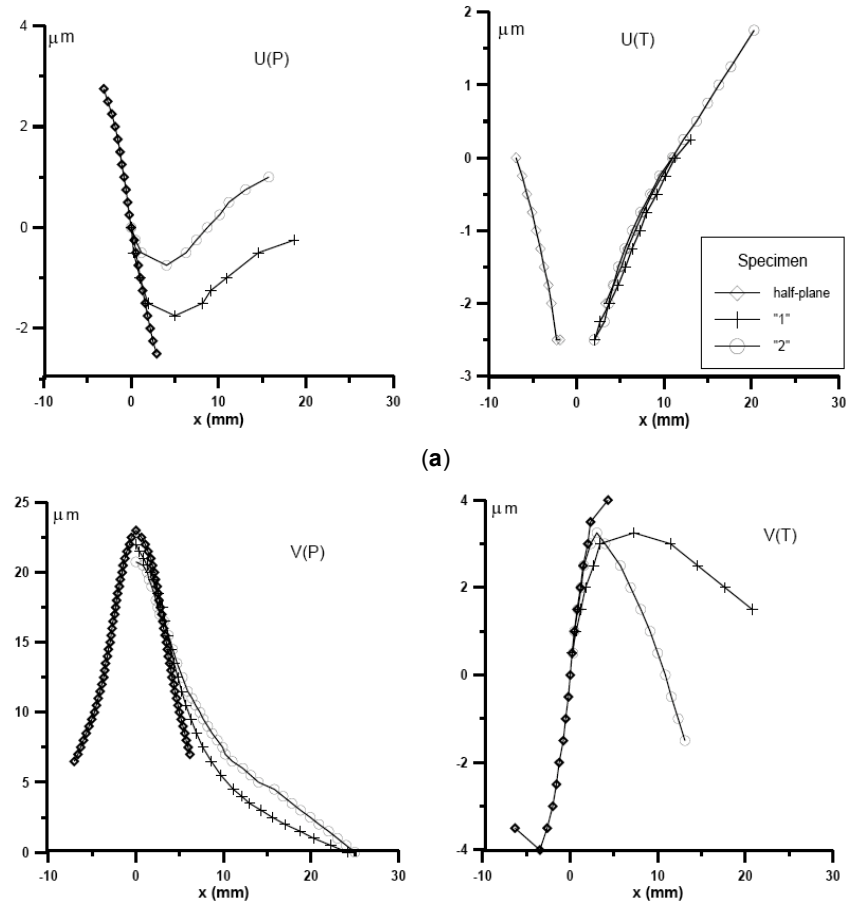

Figure 7: (**a**) U experimental data; (**b**) V experimental data; (--◊-- 'half plane' specimen, --+-- '1' specimen, --o-- '2' specimen).

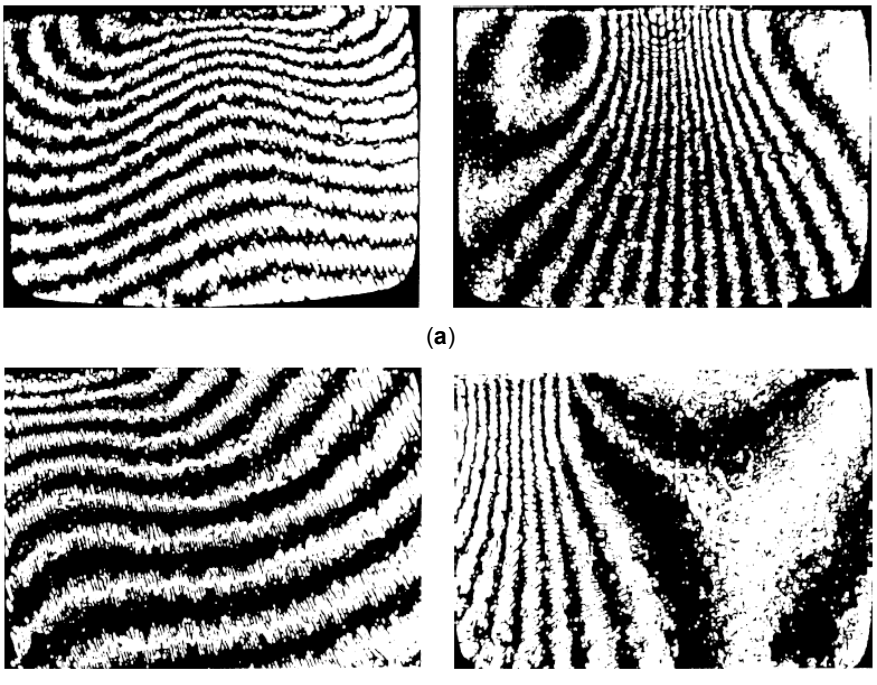

Figure 8 Continued...

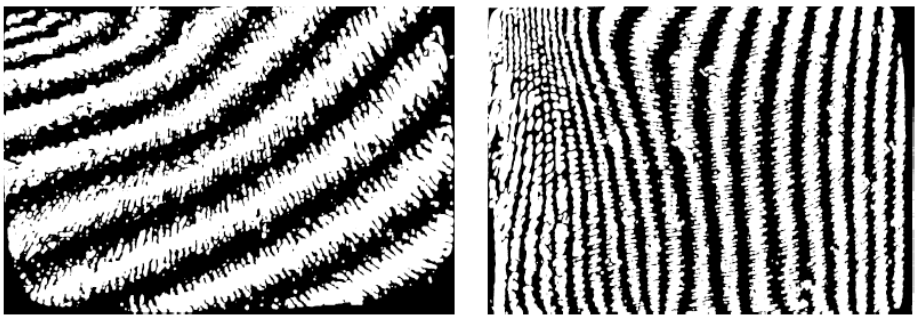

(**c**)

Figure 8: The fringes of the displacements only due to tangential load (**a**) 'half plane' specimen, (**b**)'1' specimen, (**c**) '2' specimen.

Considering the zone at the right of the center of the contact area, the trend of the U displacement reaches its minimum at the end of the contact and then increases giving tensile strains. The minimum U displacement is about -1.75 μm for the specimen 1 and the final value reached at the end of the grating is about zero. Considering the specimen 2, the minimum of the U displacement is about -0.75 μm and at the end of the grating the maximum reached is about 1 μm with a slightly increasing trend. This value approaches the theoretical half value of the total elongation of the uniform elastic bar compressed by to equal and opposite forces given by the equation (6), i.e. 2.92 μm. This consideration clarifies the reason why the half plane solution is not appropriate for the ε_x field. Even for specimen thickness of practical use (b/a >5), the global behavior must comply to the beam theory with divergent remote displacements, while in the contact area the ε_x must be compressive.

When the tangential loads are applied, the technique used allows to obtain fringes of the displacements that are only due to this additional load. These fringes are shown for all cases considered in Figure **8**. Although it is difficult to obtain a very accurate estimate at the edge of the contact area of the U displacements, indeed the differences between the specimens are negligible in the remaining zone. This implies a marginal effect of the thickness considered (b/a >5) on the stresses induced by tangential load. The superposition of the half plane strain due to the tangential load only with the strains on the finite thickness bar due to the normal load only leads to an acceptable evaluation of the tensile strain at the edge of the contact area. This confirms the conclusions obtained in the numerical study of the same problem [12].

5. CONCLUSIONS

The work carried out has shown that the use of the half-plane model loaded by normal and tangential loads in fretting fatigue tests performed on specimens of practical use can underestimate the tensile stress component, which is important for any crack initiation and propagation model. The super moiré technique has been chosen because it allows a simple separation of the contribution to the strains of normal and tangential loads. Although the resolution obtained in the tests is inadequate for obtaining the pattern of the shear stresses within the contact area, and in particular the recognition of the slip-stick separation point, some conclusions can be drawn, that have important implications in the interpretations of fretting fatigue tests:

a) The tensile stresses caused by the normal load are present even for specimens of practical use (i.e. having the ratio between the thickness and the contact area half width greater than 5), and this is due to the differences in the constraints with respect to the idealized half plane model;

b) The tensile stresses due only to the tangential load appear to be independent upon the thickness of the bar, hence the half plane model seems to be adequate for an approximate estimate of these stresses. For specimens of practical use the half plane model is adequate for the calculation of the surface tractions and the subsurface stresses, considering the bulk tension in the bar, which include the tensile stresses induced by the normal load.

REFERENCES

[1] Nowell D and Hills DA. Mechanics of fretting fatigue testing. Int J Mech Sci 1987; 29(5): 355-365. http://dx.doi.org/10.1016/0020-7403(87)90117-2

[2] Smith JO and Liu CK. Stress due to tangential and normal loads on an elastic solid. Trans ASME, Series E. J Appl Mech 1953; 20: 157-166.

[3] Mindlin RD and Derenciewicz H. Elastic spheres in contact under varying oblique forces. Trans ASME, Series E. J Appl Mechanics 1953; 20: 237-245.

[4] Poritsky H. Stresses and deflections of cylindrical bodies in contact with application to contact of gears and of locomotive wheels. Trans ASME, Series E. J Appl Mechanics 1950; 72: 191-201.

[5] Bentall RH and Johnson KL. An elastic strip in plane rolling contact. Int J Mech Sci 1968; 10: 637-663. http://dx.doi.org/10.1016/0020-7403(68)90070-2

[6] Nowell D, Hills DA, "Contact problems incorporating elastic layers", Int. J. Solids and Struct 1988; 1: 105-115. http://dx.doi.org/10.1016/0020-7683(88)90102-3

[7] Fellows LJ, Nowell D, Hills DA. Wear 1995; 185: 235-238. http://dx.doi.org/10.1016/0043-1648(95)06613-6

[8] Post D. Moiré Interferometry: Advances and Application. Experimental Mechanics 1991; 31(3): 276-280. http://dx.doi.org/10.1007/BF02326072

[9] Trentadue B, Sun WM and Pappalettere C. Study of a super-moiré interferometry by means of an image processing program. ÖIAZ Journal 1995; 295-299.

[10] Demelio G, Pappalettere C, Sun WM and Trentadue B. Experimental stress analysis for contact problems with friction by means of Moiré-interferometry. Photomécanique 95, Cachan, Paris 14-15-16 Mars, 1995.

[11] Timoshenko and Goodier. Theory of elasticity. McGraw Hill, New York 1970.

[12] Ciavarella M, Demelio G and Monno G. Studio numericio dello stato tensionale in un problema di contatto con attrito. XXIV AIAS Conference, Parma, Italy 1995; 318-329: 27-30 Settembre.

Received on 08-06-2015 Accepted on 30-07-2015 Published on 31-12-2015

DOI: http://dx.doi.org/10.15377/2409-9848.2015.02.02.1